Impact of increased UV curing time on the curing depth of photosensitive resins for 3D Printing

Callum Guttridge
University of Limerick
Alice Shannon
University of Limerick
Aidan O'Sullivan
University of Limerick
Kevin J. O'Sullivan
University of Limerick
Leonard W. O'Sullivan (leonard.osullivan@ul.ie)
University of Limerick

Research Article

Keywords: 3D printing, photosensitive resin, post-processing, biocompatible, vat-polymerisation

Posted Date: May 11th, 2022

DOI: https://doi.org/10.21203/rs.3.rs-1626243/v1

Abstract

Background

3D printing (3DP) photosensitive resins are commonly used to produce patient-specific solutions in the fields of medicine and dentistry. These resins are toxic in their liquid state. To ensure that all resin has solidified and parts are safe for use, post-processing must be carried out after printing. Parts are first washed in IPA, allowed to dry, and then post-cured under ultra-violet light (UV), and sometimes heat. As 3DP is commonly utilised for its ability to create custom and rapid solutions, it is expected that a different geometry will be produced almost every time. Currently, post-processing guidance is supplied specific to a material, with the caveat that post-curing times should be extended for larger or complex parts. The aim of this study was to assess the effect of extending post-curing times for photosensitive resin printed parts.

Method

Two commercially available vat-polymerisation 3DP systems were used to print hollow 60mm diameter spheres. Two opaque white, two opaque black, and two translucent amber resins were used. The spheres were filled with liquid resin, then UV post-cured at intervals of 100, 200, 300, 400 and 500% of the recommended guidance. The spheres were sectioned along the centreline and radial measurements taken of the cured depth.

Results

The results showed that both translucent amber materials cured to full depth at the 100% interval, whereas none of the white or black opaque materials cured to full depth, even at 500% of the recommended guidance.

Conclusions

This suggests opacity has a considerable effect on the depth of cure in photosensitive resins, and that the use of opaque resins increases the possibility of uncured resin remaining inside parts.

1. Introduction

The potential of 3D printing (3DP) was first recognised in the medical community as early as the 1990's (1–3). In the last two decades there has been a significant increase in the adoption of 3DP being used to directly treat patients (4, 5). 3DP offers customised and rapid solutions whilst reducing manufacturing time and costs (6). Fields such as surgery, biomedicine, dentistry, and microfluidics utilise 3DP as a manufacturing method often at the point-of-care (7–10). However, 3DP is still relatively novel with

regards to many of its applications, particularly when used to directly treat patients. The framework for regulation is still in its infancy and is yet to be fully established (11–13). It is therefore important to evaluate current practices and procedures to ensure the safety of users and end users.

Vat-polymerisation 3DP methods are often favoured over other methods for characteristics such as dimensional accuracy, isotropy, cleanability, and the wide availability of industry specific materials (4, 14–16). Vat-polymerisation 3DP uses UV light to change the state of the liquid resin to a solid, layer by layer, to form a 3D part. When exposed to UV light, photo-initiators in the resin react and form polymer chains from oligomers and monomers: a process termed photo-crosslinking (7, 17, 18). The UV light is projected from a focussed energy source such as a refracted laser (Stereolithography [SLA]), projector (Digital Light Processing [DLP] or Digital Light Synthesis™ [DLS™]), array light source and digital mask (Masked-Stereolithography [MSLA]), or from a masked projected light source or digital screen (Liquid Crystal Display [LCD]). The light source cures a 2D cross section of the 3D model between the vat membrane and the build platform, the z-axis moves the bed away from the membrane to allow resin to flow back, and this process then repeats to form the next layer until the part is complete (17, 19, 20).

The intention of post-curing is to ensure that the semi-cured resin in the model has fully undergone the transition from a liquid to a solid (21).Vat-polymerisation printed parts are removed from the machine in their ‘green’ state and so require post-processing to ensure all semi-cured resin is fully cured, and that any liquid remnants are washed off. Materials are supplied with instructions for use and information for users regarding best practices for post-processing. Typically, isopropyl alcohol (IPA) or a solution such as tripropylene glycol monomethyl ether, is firstly used to remove liquid remnants. Washing is carried out manually or in an automated wash station specifically designed for washing vat-polymerised parts. Parts are allowed to air dry and then placed into a UV curing tank where they are exposed to a specific wavelength of UV light and sometimes heat, for a prescribed duration.

Post-processing is a vital step for vat-polymerisation 3DP methods as photosensitive resins are toxic in their liquid state (17, 22). When supplied, the material safety data sheet informs the user that the raw resin is toxic and that improper use may cause an immunological response from the host (23, 24). It is inferred from the manufacturer’s guidance that after post-processing parts will be free from harmful liquid resin and safe for the intended application. However, several recent studies have found that even after post-processing has occurred, harmful toxic leachates have been identified on parts printed using photosensitive resins (17, 22, 25–27).

Post processing guidance supplied by the manufacturer is material specific and so applies universally to all geometries that may be produced with that material. As a method, 3DP is utilised for its ability to create bespoke and complex parts. Therefore, a printer is expected to produce different geometries almost every time it is used. As such, some parts may feature thicker or complex geometries and may feature internal chambers, channels, and areas that will be shadowed from the UV light source during post-curing. Material manufacturers recommend extending post-curing durations for parts that are large or feature complex geometries, and for the user to apply their own judgement for post-processing

technique. This suggests that post-processing guidance should be customised in relation to part geometry and that due diligence must be performed to ensure that the process is successful in curing parts and any liquid resin remnants.

The aim of this study was to evaluate the effects of extending post-curing by increasing intervals of the recommended post-curing guidance for photosensitive resins using their respective curing systems.

2. Method

2.1 3D printer technology

One DLP printer, the Fig. 4 Standalone (3D Systems, USA), and one SLA 3D printer, Form 3B (FormLabs, USA) were used for this study. The systems were chosen as they are both commercially available, offer a comprehensive range of specifically engineered functional and biocompatible materials, and have their own proprietary post-processing equipment supplied with specific post processing guidance. The Fig. 4 uses the LC-3DPrint Box UV Post-Curing Unit, for curing parts, and the LC-3DMixer for mixing the resin bottles prior to printing. The Form 3B uses the FormCure for curing parts and the FormWash for washing parts.

2.2 Test model

The test model used was a hollow 60mm diameter sphere with a nominal wall thickness of 2mm. The sphere featured a filling hole of diameter 4.4mm with a 45^{o} chamfer. The hole was designed to fit a 25ml syringe (Terumo, Japan) whilst also allowing air to escape (Fig. 1a, b). A plug for the filling hole was also designed. The plug had a 4.4 x 1.2mm shaft attached to an 8 x 8 x 2mm square pedestal used to balance the sphere during curing and to orientate the sphere during cutting (Fig. 1c, d).

The models were drawn in SolidWorks 2020 (Dassault Systems, USA) then exported as a standard tessellation language (.STL) file to the appropriate slicing program. The slicing software for the Fig. 4 system is ‘3D Sprint’ (3D Systems, USA) and for the Form 3B system, ‘Preform’ (Formlabs, USA).

Figure 1: Sphere and plug dimensions

2.3 Materials

Six materials were chosen for the study, two opaque white, two opaque black and two translucent ambers (Formlabs White, Formlabs Black, Formlabs BioMed Amber, Fig. 4 MED-WHT 10, Fig. 4 Pro BLK 10 and Fig. 4 MED-AMB 10). Black and white pigments were chosen as they were expected to produce the broadest range of results based on their light transmittance (28, 29). The translucent resins were chosen as they would allow light to pass with minimal refraction (30). Where possible biocompatible materials were chosen. At the time of the experiment, the equivalent coloured resin was not available as a biocompatible, so the non-biocompatible version was used (i.e., FormLabs Black, FormLabs White).

2.4 Sample size

Five spheres were printed for each material, one for each time interval (100%-500%), giving a planned sample size of n = 30. However, as the translucent resins cured fully at 100% the other samples were not further considered, giving an actual sample size of 22.

2.5 Material and machine preparation

Prior to printing on the Fig. 4 system, resin bottles were placed on the 3D Systems LC-3D Mixer and rolled for 60 minutes for PRO-BLK 10 and 150 minutes for MED-WHT 10 Rolling is not required for the MED-AMB 10 as per the manufacturers guidance. The Formlabs material did not require pre-mixing. Prior to each print, print beds were also inspected and cleaned as prescribed.

For slicing, a layer height of 50µm was chosen on Preform and 3D Sprint. The 'standard' option was selected in 3D Sprint. During the slicing process, care was taken to remove all internal supports that were generated inside the spheres and only one sphere and one plug was printed at a time. Spheres were orientated with the fill hole towards the bed to counteract an airlock being created between the part and the bed. The plug was printed with the square face away from the bed to avoid a rough finish.

2.6 Washing

As washing was not a variable of this experiment, a standard protocol was used to ensure consistency. To remove liquid resin from the parts, spheres were filled with 20ml of IPA using a 25ml syringe, shaken for ten seconds, and then allowed to drain. This was repeated until the liquid draining from the part was visibly clear. A brush was used to clean the outside of the spheres, and the plugs. The IPA was changed between each material to avoid contamination. After washing, parts were left to air dry for 60 minutes.

2.7 Filling of spheres

Each sphere was filled using a 25ml syringe with its corresponding resin to the brim and allowed to overflow, then sit for ten minutes to allow any air bubbles to form at the surface. If necessary, the sphere was topped up with resin, then the plug inserted into the filling hole. Cyanoacrylate (M5100 H.B. Fuller, USA) was used to secure the plug in place. Once applied it was left to dry for ten minutes, as recommended.

2.8 Post-curing

Spheres were placed in the centre of the appropriate curing tank standing upright on the square faced plug. Spheres were cured at 100, 200, 300, 400 or 500% of the recommended durations, as provided by the manufacturers (Table 1).

Table 1
Manufacturer curing guidance

Material	Curing
Formlabs White	100% = 60 min @ 60°c
Formlabs Black	100% = 60 min @ 60°c
Formlabs Biomed Amber	100% = 30 min @ 70°c
Figure 4 MED-WHT 10	100% = 60 minutes
Figure 4 PRO-BLK 10	100% = 90 minutes
Figure 4 MED-AMB 10	100% = 60 minutes

2.9 Draining

After curing two holes were drilled into the spheres to drain any liquid resin remaining inside. A drilling jig was designed and printed on an FDM printer (Raise 3D N2+, USA) in PLA (Polymaker, Netherlands) filament. The jig was designed so that both holes could be drilled into the sacrificial half of the spheres (see 'cutting section' below) and penetrate exactly to the centre of the sphere. A 5mm drill bit and cordless drill were used to create the two holes. The drilling jig is shown in Fig. 2a. The location slot for the sphere pedestal can be seen in Fig. 2b. The spheres were left to drain into a waste container for ten minutes. They were then washed using the same technique described previously and left to dry for 60 minutes.

Figure 2: Drilling jig

2.10 Cutting spheres

A cutting jig was designed so that the cut would be offset by 2mm from the centre of the sphere allowing the larger hemisphere to be sanded back to its mid-point, as shown in Fig. 3a. The smaller hemisphere featured the plug and drainage holes and which discarded after cutting (sacrificial half).
Spheres were placed into the jig with the square pedestal slotted into the extruded square gap, this was to prevent spinning during cutting. The spheres were cut inside the jig using a band saw. The cutting jig and thumbscrews were printed in Vero Clear resin and the gaskets were printed in Tango Black on a Connex 500 polyjet printer (Stratasys, Israel). A range of sandpapers, 240 through 1500 grit, were used to finish the flat face of each hemisphere.

Figure 3: Cutting jig

2.12 Measurement of wall thickness

An alignment tool and a measurement jig were designed and printed on the FDM printer to aid in the scanning process. The jig and tool were sat against the straight edge of the scanner (Fig. 4a) with the hemisphere faced down on the scanner. The tool was used to centre the hemisphere in the jig (Fig. 4b) and thereafter removed (Fig. 4c) leaving an 8mm gap offset from each side of the hemisphere. Scans were taken at 600DPI and exported to a media drive as a JPEG file (Brother, MFC-J6510DW, Japan). As the black and amber hemispheres did not show up clearly when scanned, white paint was applied to the sectioned face using an airbrush to increase the contrast.
Figure 4: *Measurement jig and alignment tool*

The scanned images were cropped to the inner edge of the measurement jig, leaving an 8mm gap tangent to the sphere and the two prongs of the measurement jig visible. The two prongs of the measurement jig (60mm apart) were used as a reference dimension. Image J (Rasband, W.S., ImageJ, USA) was used to convert the scans to 32-bit greyscale and the contrast adjusted to maximum to ensure all of the cured depth was detected during measurement.

A radial measurement plugin for ImageJ was used to take 360 radial measurements from the image. The images were cropped purposefully so that the plugin measures from the centre of the hemisphere

each time. The arm then rotates, recording points from the outer printed edge of the hemisphere, to the inner post-cured depth using the grayvalues to determine start and end points. The settings used for the macro can be seen in Table 2.

Table 2
Settings for ImageJ radial measurement macro

Settings:	**Values:**
Radius of Interest (ROI)	35
Coordinates for X (mm)	37.5
Coordinates for Y (mm)	37.5
Start Angle	1
Last Angle	360
Angle Increment	1
Minimum Grayvalues	150 (100 for Black and Amber)
Maximum Grayvalues	250 (300 for Black and Amber)

3. Results

Images of the cross-sectioned spheres are shown in Fig. 5 and the results of the radial measurement data reported in Table 3. Three out of four of the opaque resins showed an increase in curing depth when exposed to extended curing times, but none cured to full depth. Both translucent amber materials cured to full depth at the first interval of post-curing. Figure 6 highlights the difference in cured depth between the opaque and translucent materials.

From the nominal depth to the cured depth recorded at 500%, the Fig. 4 MED-WHT 10 showed an increase in maximum cure depth of 8.72mm and a mean increase of 8.06mm (Table 3). The internal circumference of the cured depth is visually noncircular after the 100% interval and is emphasized more with each interval (Fig. 5a). The external shape remained circular and no deformation was noted.

From the nominal depth to the cured depth recorded at 500%, the Fig. 4 PRO-BLK 10 showed an increase in maximum cure depth of 2.15mm and a mean increase of 1.74mm (Table 3). The shape of the cured depth is visually non-circular after the 100% interval (Fig. 5b) and more emphasized with each interval thereafter. A change in the external shape can be seen after the 300% interval where the model began to deform and become non-spherical.

The Fig. 4 MED-AMB 10 resin cured to full depth at the 100% interval (Fig. 5c). Accordingly, no further curing intervals were assessed.

From the nominal depth to the cured depth recorded at 500%, the Formlabs White resin showed an increase in maximum cure depth of 6.46mm and a mean increase of 6.22mm (Table 3). No change in shape was noted in the internal or external circumference (Fig. 5d).

The Formlabs Black resin showed no increase in cure depth from having the curing time extended. The maximum cure depth of each sphere was within ± 0.09mm, and the mean cure depth within ± 0.05mm (Table 3), it is expected that the value shown is the error of margin in the printers accuracy. No change in shape was noted in the internal or external circumference (Fig. 5e).

The Formlabs BioMed Amber cured to the full depth at the first interval of 100%, as it could not cure any further, no more intervals were tested. A large irregular shaped cavity was found in the centre of the sphere (Fig. 5f). The sphere was drilled to release any liquid resin still held inside the centre, but none was found. The 100% interval was repeated two more times to check for user error (Fig. 7b, c). No change in shape was noted in the external circumference.

Table 3
Sphere cured depth by time interval

Figure 4 Resins					
MED-WHT 10					
Cure Interval/Time	**100% (60 Min)**	**200% (120 Min)**	**300% (180 Min)**	**400% (240 Min)**	**500% (300 Min)**
Max Thickness (mm)	3.94	6.82	7.36	9.99	10.72
Min Thickness (mm)	2.65	4.91	6.01	8.05	9.45
Mean Thickness (mm)	3.44	5.56	6.62	9.15	10.06
SD (mm)	0.07(± 1%)	0.19 (± 1.7%)	0.29 (± 2.1%)	0.54 (± 2.9%)	0.41 (± 2%)
PRO-BLK 10					
Cure Interval/Time	**100% (90 Min)**	**200% (180 Min)**	**300% (270 Min)**	**400% (360 Min)**	**500% (450 Min)**
Max Thickness (mm)	2.2	2.54	3.09	3.64	4.15
Min Thickness (mm)	1.90	1.99	2.16	2.83	3.34
Mean Thickness (mm)	2.03	2.16	2.66	3.17	3.74
SD (mm)	0.05(± 1.2%)	0.1(± 2.3%)	0.19 (± 3.5%)	0.18 (± 2.8%)	0.19 (± 2.5%)
MED-AMB 10					
Cure Interval/Time	**100% (60 Min)**				
Max Thickness (mm)	30.56				
Min Thickness (mm)	28.73				
Mean Thickness (mm)	29.55				
SD (mm)	0.58 (± 0.9%)				
Formlabs Resins					
White					

Figure 4 Resins					
Cure Interval/Time	**100% (60 Min)**	**200% (120 Min)**	**300% (180 Min)**	**400% (240 Min)**	**500% (300 Min)**
Max Thickness (mm)	4.15	5.97	6.44	7.4	8.46
Min Thickness (mm)	3.26	4.62	5.88	6.9	7.83
Mean Thickness (mm)	3.72	5.37	6.15	7.14	8.22
SD (mm)	0.21 (± 2.8%)	0.14 (± 1.3%)	0.12 (± 0.9%)	0.12 (± 0.8%)	0.14 (± 0.8%)
Black					
Cure Interval/Time	**100% (60 Min)**	**200% (120 Min)**	**300% (180 Min)**	**400% (240 Min)**	**500% (300 Min)**
Max Thickness (mm)	2.24	2.24	2.33	2.28	2.28
Min Thickness (mm)	1.95	1.94	1.9	1.99	1.95
Mean Thickness (mm)	2.11	2.06	2.06	2.08	2.08
SD (mm)	0.04 (± 0.9%)	0.05 (± 1.2%)	0.05 (± 1.2%)	0.04 (± 0.9%)	0.04 (± 0.9%)
BioMed Amber					
Cure Interval/Time	**100% (30 Min)**				
Max Thickness (mm)	23.8*				
Min Thickness (mm)	19.27*				
Mean Thickness (mm)	22.33*				
SD (mm)	1.28 (± 2.8%)*				

Figure 6: Mean curing depth of all resins

Figure 7: Biomed amber cavitation

4. Discussion

4.1 Depth of curing

Vat-polymerisation 3DP is often utilised in the fields of medicine and dentistry to produce medical devices that are used to directly treat patients. Vat-polymerisation systems use a photosensitive resin that transitions from a liquid to a solid during exposure to UV light. Vat-polymerisation systems use a focussed UV energy source to construct the model, the conversion rate of the resin at this stage is > 50% and so requires post-processing to achieve a rate of > 90% (18). As photosensitive resins are toxic in their liquid state, post-processing is vital to ensure the parts are finished and are safe for use. Post-processing guidance is provided by the resin manufacturers. Manufacturers recommend extending post-curing times for parts that feature large or complex geometries, however there is a general lack of specific guidance in this respect. This study was performed to assess the effects of extending post-curing times on a selection of photosensitive resins. The results of the current study identified that extending post-curing times increased the cure depth of the resins, but that the effects varied considerably between resin opacities.

In this study, two translucent and four opaque photosensitive resins were post-cured at extended intervals of the prescribed post-curing guidance provided by the manufacturer, to test how cure depth would be affected. Both translucent resins cured to their full depth at 100% of the recommended guidance, whereas none of the opaque materials cured to full depth even at 500%. Of the opaque resins, the two white resins had the deepest recorded cure depths. From nominal depth to 500%, the Fig. 4 MED-WHT 10 gained a mean increase of 8.06mm, this was followed by the Formlabs White resin with a mean increase of 6.22mm. The two black resins showed the smallest increase in cure depth, with the Fig. 4 PRO-BLK 10 resin increasing by 1.74mm and the Formlabs Black resin showing no discernible increase at all.

The results of this study show that extending post-curing times is highly variable, and is dependent on the opacity of the resin. Figure 6 demonstrates how much of a difference opacity makes. After extending post-curing times to 500%, most of the opaque resins were able to cure further, but none cured to full depth. Compared with the translucent resins that both cured to full depth after just 100% of their recommended guidance. As photosensitive resins require exposure to UV light to transition from a liquid to a solid, understandably, opacity has had a considerable effect on the depth of cure. Whilst the method used in this study is unlikely to be repeated by a user, it is designed to replicate uncured resin that may be left inside a large or complex printed geometry. The geometry used in this experiment is relatively simple and would not be considered complex, or large in relation to the capability of the machines. It could be expected that parts with features such as, thicker walls, channels, threads, and other captive elements would require a post-curing interval past 500% to achieve relative cure depth.

Extending post-curing times showed high variation in cure depth for the opaque resins. For these types of material, users may want to consider introducing limitations for part size and complexity, and to consider breaking designs down into smaller sub-assemblies. Ultimately, the responsibility is on the user to ensure the parts are fully cured and safe for use, by firstly carrying out the prescribed post-processing guidance and then validating its success with regards to the unique geometry they are producing. When possible,

users should seek to use translucent resins for producing medical devices that will be used to directly treat patients to increase the cure depth achieved during post-processing.

4.2 Potential impact on biocompatibility

Of the materials used in this study, four out of six are marketed as biocompatible. Biocompatible refers to the materials ability to not cause an immunological response to the host at the point of contact within the stated time period e.g. 24-hour skin contact, 12-hour mucosal membrane contact (23, 24). It is likely that materials marketed with these characteristics will be chosen by some users to produce medical devices for human use. In this study, the Fig. 4 MED-WHT 10, Fig. 4 PRO-BLK 10, Fig. 4 MED-AMB 10 and the Formlabs BioMed Amber are all certified in accordance with ISO 10993-5 (tests for in vitro cytotoxicity) and 10993-10 (tests for irritation and skin sensitization). In addition, Formlabs BioMed Amber is also certified under ISO 10993-1 (evaluation and testing within a risk management process)(31).

The results presented here suggest that caution is required when using opaque resins for biocompatible applications as the penetration of UV light is compromised, potentially leading to semi-cured or uncured resin remaining inside large parts, or those with complex internal geometries. To ensure the safety of end users the amount of cytotoxic remnants inside a printed part must be reduced. Whilst it is known that post-curing under UV light largely mitigates the toxicity of photosensitive printed parts (22), other methods have proven successful. Studies performed by Macdonald et al (26) and Alifui-Segbaya et al (17) showed that soaking photosensitive resin printed parts in ethanol significantly reduced cytotoxicity levels. Similarly, Inoue and Ikuta showed that heating parts to 225^{o}C successfully reduced the cytotoxicity of photosensitive resin printed parts (32). These methods may be useful for biocompatible devices that require complex or large geometries, and/or must be printed in opaque resins. When extending part exposure to heat, irradiation or solvents, users must be aware of the potential for detrimental side effects to parts, as highlighted by Kim et al (14), where the flexural modulus of parts began to decrease after extending post-curing times, in some cases. Similarly, Xu et al (33) found that the flexural strength of photosensitive resin printed parts decreased with the extension of post-washing times. When employing biocompatible photosensitive resins for medical devices, users should seek to use quality certified materials from reputable manufacturers that are appropriate for the devices intended use (34). If possible, users should use translucent resins, and perform due diligence to ensure that post-processing has been successful and not detrimental to the mechanical or biocompatible properties of their device.

4.3 Visual changes

Visual changes of the samples were noted with regards to shape. An irregularity in the internal circumference was noted across the Fig. 4 MED-WHT samples, and also for the 200% interval onwards Fig. 4 PRO-BLK samples, where the internal circumferences become noncircular. The internal circumferences of the Formlabs Black and White resins are noticeably more circular than the Fig. 4 MED-WHT and PRO-BLK resins. The irregularity of the internal shape was also noted in the variability of the measured diameters. The two opaque Fig. 4 resins had higher standard deviations than the Formlabs resins in most instances. A possible explanation for the variability may be due to the difference between

the respective curing tanks used. The proprietary curing tank supplied by Formlabs (Formcure) has a platform that turns parts slowly whilst exposed to thirteen 9.1W multi-directional LEDs. The Fig. 4 recommended curing box (LC-3DPrint Box) does not have a revolving platform. The LC-3DPrint Box has twelve fluorescent bulbs that differ in wavelength: six are 18W 71 colour and six are 18W 78 colour, with the bulbs alternating consecutively. The two bulb types produce different wavelengths of UV giving a full UV spectrum from 300-550nm. The change in internal circumference might be due to being exposed to different UV wavelengths from different directions on a stationary platform.

The BioMed Amber featured an irregular shaped cavity inside the sphere. No liquid resin was found inside the cavity after sectioning; the process was repeated a further two times to ensure it was not the result of user error. In the first and second run, cavities formed in the centre of the sphere (Fig. 7a, b), in the third run, the cavity was found offset to the centre (Fig. 7c). It is proposed that the cavities may be the result of cavitation inside the sphere. As the temperature of the resin increased and it solidified within the captive space, it reached a static pressure below the liquids vapour pressure, creating pockets of vapour that were then captured in the resin as it solidified (35, 36). This result is specific to the method used in this study and is not expected to occur under normal printing conditions.

4.4 Limitations

A study performed by Guttridge et al (34) identified 130 biocompatible photosensitive resins, as the cost and time of printing, filling and post-curing was considerable, only 6 materials were chosen for this experiment. For the same reason, only one run of each interval was tested.

This study was limited to a single geometry model. It is expected that other geometries and sizes will produce different results. The geometry used was selected to show the best results for radial measuring, and to cure evenly when placed in the centre of the respective curing tank.

As the materials used in this study are photosensitive, care was taken to keep samples out of direct light between printing, filling and draining. It is possible that during processes parts were exposed to natural and unnatural light.

5. Conclusion

Photosensitive 3DP resins are often used to produce custom devices in the fields of medicine and dentistry. These resins are toxic in their liquid state so post-processing is required to ensure that all liquid resin transitions to a solid. Post-processing guidance supplied with resins typically detail that post-curing times should be increased for larger or more complex parts, however specific detail in this respect is not ordinarily provided.

This study evaluated the effects of extending post-curing times relative to duration in the associated material guidance documentation. The results showed that whilst curing depth increased with extended UV exposure for most resins, there were large differences between resins of different opacities. The opaque resin did not cure fully at five times the recommended guidance, whereas translucent resins cured

to full depth at the recommended guidance. Users should exercise caution when using opaque resins in particular to ensure they are fully cured. Users might consider using translucent resins for devices where full curing is important, in particular for medical applications including those that require biocompatibility. There is a need for further research into the efficacy of current guidance regarding post-processing of photosensitive resins used in 3DP. Users should consider developing and validating their post-processing techniques to avoid any potential adverse effects to end users.

Glossary

3DP – 3D Printing

DLP – Digital Light Processing

DLS^{TM} – Digital Light Synthesis^{TM}

GMP – Good Manufacturing Practices

SLA – Stereolithography

STL – Standard Tessellation Language

UV – Ultra Violet

Declarations

Availability of data and materials: Data are available under reasonable request from the corresponding author.

Competing interests: The authors declare that they have no competing interests.

Funding: This publication has emanated from research supported by Science Foundation Ireland (SFI) under Grant Numbers SFI 16/RC/3918 co-funded by the European Regional Development Fund.

Author's contributions: CG was the major contributor to the writing of the manuscript, performed experimental work and analysis. AS contributed to the experimental design and results from a materials perspective. AOS, KOS and LOS contributed to the writing of the design of the experiment, analysis of the results and writing of the manuscript. All authors read and approved the final manuscript.

Acknowledgements: Not applicable

Ethics approval: Not applicable

References

1. Cima M, Sachs E, Cima L, Yoo J, Khanuja S, Borland S, et al., editors. computer-derived microstructures by 3D Printing: Sio-and Structural Materials. 1994 International Solid Freeform Fabrication Symposium; 1994.
2. Wu BM. Microstructural control during three dimensional printing of polymeric medical devices: Massachusetts Institute of Technology; 1998.
3. Tack P, Victor J, Gemmel P, Annemans L. 3D-printing techniques in a medical setting: a systematic literature review. Biomed Eng Online. 2016;15(1):1–21.
4. Kermavnar T, Shannon A, O'Sullivan KJ, McCarthy C, Dunne CP, O'Sullivan LW. Three-dimensional printing of medical devices used directly to treat patients: a systematic review. 3D Printing and Additive Manufacturing. 2021;8(6):366–408.
5. Tack P, Victor J, Gemmel P, Annemans L. 3D-printing techniques in a medical setting: a systematic literature review. Biomed Eng Online. 2016;15(1):115-.
6. Ventola CL. Medical Applications for 3D Printing: Current and Projected Uses. P&T (Lawrenceville, NJ). 2014;39(10):704 – 11.
7. Bagheri A, Jin J. Photopolymerization in 3D Printing. ACS Applied Polymer Materials. 2019;1(4):593–611.
8. Jovicic MS, Vuletic F, Ribicic T, Simunic S, Petrovic T, Kolundzic R. Implementation of the three-dimensional printing technology in treatment of bone tumours: a case series. International Orthopaedics.7.
9. Lin M, Firoozi N, Tsai C-T, Wallace MB, Kang Y. 3D-printed flexible polymer stents for potential applications in inoperable esophageal malignancies. Acta biomaterialia. 2019;83:119–29.
10. Masaki A, Toru Y, Naomi I-K, Fumihiko U, Takaaki I, Kenji Y, et al. Mandibular reconstruction using plates prebent to fit rapid prototyping 3-dimensional printing models ameliorates contour deformity. Head & Face Medicine. 2014;10:1–8.
11. Pierrakakis K, Kandias M, Gritzali C, Gritzalis D, editors. 3D Printing and its regulation dynamics: The world in front of a paradigm shift. Proc of the 6th International Conference on Information Law and Ethics; 2014: Citeseer.
12. Christensen A, Rybicki FJ. Maintaining safety and efficacy for 3D printing in medicine. 3D printing in medicine. 2017;3(1):1–10.
13. Horst A, McDonald F. Uncertain but not unregulated: medical product regulation in the light of three-dimensional printed medical products. 3D Printing and Additive Manufacturing. 2020;7(5):248–57.
14. Kim D, Shim J-S, Lee D, Shin S-H, Nam N-E, Park K-H, et al. Effects of post-curing time on the mechanical and color properties of three-dimensional printed crown and bridge materials. Polymers. 2020;12(11):2762.
15. Unkovskiy A, Bui PH-B, Schille C, Geis-Gerstorfer J, Huettig F, Spintzyk S. Objects build orientation, positioning, and curing influence dimensional accuracy and flexural properties of stereolithographically printed resin. Dental Materials. 2018;34(12):e324-e33.

16. Juneja M, Thakur N, Kumar D, Gupta A, Bajwa B, Jindal P. Accuracy in dental surgical guide fabrication using different 3-D printing techniques. Additive Manufacturing. 2018;22:243–55.
17. Alifui-Segbaya F, Varma S, Lieschke GJ, George R. Biocompatibility of photopolymers in 3D printing. 3D Printing and Additive Manufacturing. 2017;4(4):185–91.
18. Kessler A, Reichl F-X, Folwaczny M, Högg C. Monomer release from surgical guide resins manufactured with different 3D printing devices. Dental Materials. 2020;36(11):1486–92.
19. Kodama H. Automatic method for fabricating a three-dimensional plastic model with photo-hardening polymer. Review of scientific instruments. 1981;52(11):1770–3.
20. Hull CW. Apparatus for production of three-dimensional objects by stereolithography. United States Patent, Appl, No 638905, Filed. 1984.
21. Piedra-Cascón W, Krishnamurthy VR, Att W, Revilla-León M. 3D printing parameters, supporting structures, slicing, and post-processing procedures of vat-polymerization additive manufacturing technologies: A narrative review. Journal of Dentistry. 2021;109:103630.
22. Oskui SM, Diamante G, Liao C, Shi W, Gan J, Schlenk D, et al. Assessing and reducing the toxicity of 3D-printed parts. Environmental Science & Technology Letters. 2016;3(1):1–6.
23. Remes A, Williams DF. Review: Immune response in biocompatibility. In: Williams DF, editor. The Biomaterials: Silver Jubilee Compendium. Oxford: Elsevier Science; 1992. p. 79–91.
24. Barrère F, Mahmood TA, de Groot K, van Blitterswijk CA. Advanced biomaterials for skeletal tissue regeneration: Instructive and smart functions. Materials Science and Engineering: R: Reports. 2008;59(1):38–71.
25. Rogers HB, Zhou LT, Kusuhara A, Zaniker E, Shafaie S, Owen BC, et al. Dental resins used in 3D printing technologies release ovo-toxic leachates. Chemosphere. 2021;270:129003.
26. Macdonald NP, Zhu F, Hall C, Reboud J, Crosier P, Patton E, et al. Assessment of biocompatibility of 3D printed photopolymers using zebrafish embryo toxicity assays. Lab on a Chip. 2016;16(2):291–7.
27. Walpitagama M, Carve M, Douek AM, Trestrail C, Bai Y, Kaslin J, et al. Additives migrating from 3D-printed plastic induce developmental toxicity and neuro-behavioural alterations in early life zebrafish (Danio rerio). Aquatic Toxicology. 2019;213:105227.
28. Levinson R, Berdahl P, Akbari H. Solar spectral optical properties of pigments—Part I: model for deriving scattering and absorption coefficients from transmittance and reflectance measurements. Solar Energy Materials and Solar Cells. 2005;89(4):319–49.
29. Wilson C, Gies P, Niven B, McLennan A, Bevin N. The relationship between UV transmittance and color—visual description and instrumental measurement. Textile research journal. 2008;78(2):128–37.
30. Bohren CF. Understanding colors in nature. Pigment Cell Research. 1988;1(4):214–22.
31. ISO. ISO 10993: Biological evaluation of medical devices. International Standards Organisation. 2001.
32. Inoue Y, Ikuta K. Detoxification of the Photocurable Polymer by Heat Treatment for Microstereolithography. Procedia CIRP. 2013;5:115–8.

33. Xu Y, Xepapadeas AB, Koos B, Geis-Gerstorfer J, Li P, Spintzyk S. Effect of post-rinsing time on the mechanical strength and cytotoxicity of a 3D printed orthodontic splint material. Dental Materials. 2021;37(5):e314-e27.
34. Guttridge C, Shannon A, O'Sullivan A, O'Sullivan KJ, O'Sullivan LW. Biocompatible 3D printing resins for medical applications: a review of marketed intended uses, biocompatibility certification, and post-processing guidance. Annals of 3D Printed Medicine. 2021:100044.
35. Franc J-P, Michel J-M. Fundamentals of cavitation: Springer science & Business media; 2006.
36. Moussatov A, Granger C, Dubus B. Cone-like bubble formation in ultrasonic cavitation field. Ultrasonics Sonochemistry. 2003;10(4):191–5.

Figures

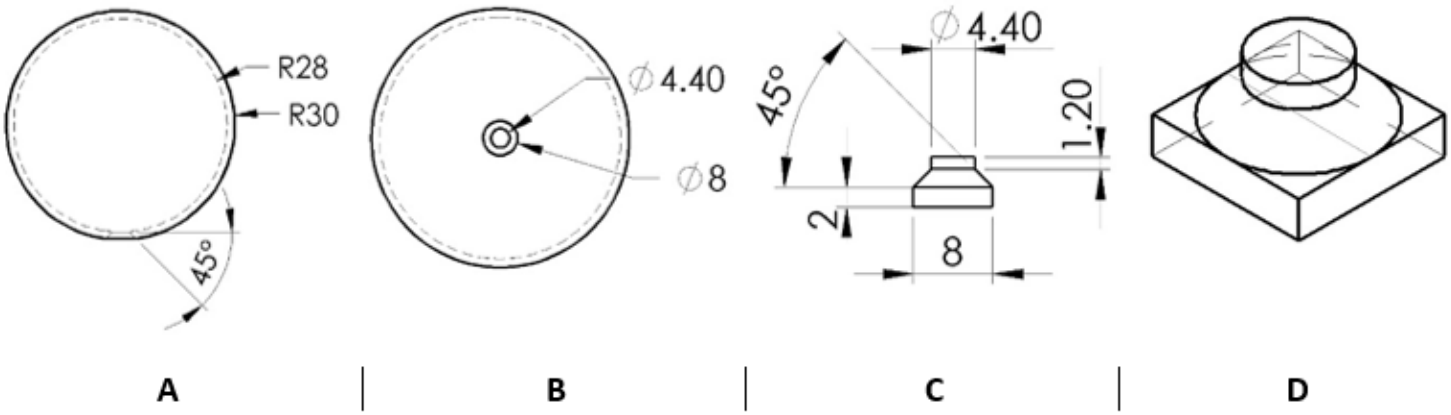

Figure 1

Sphere and plug dimensions

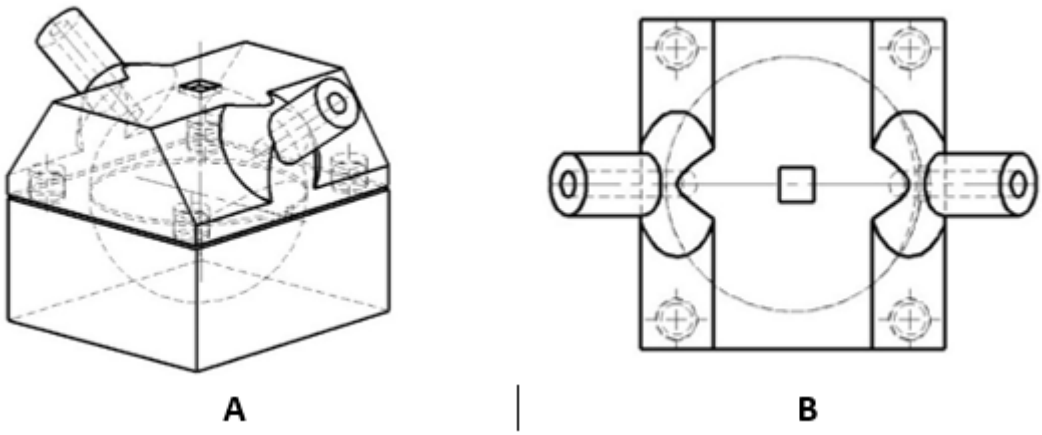

Figure 2

Drilling jig

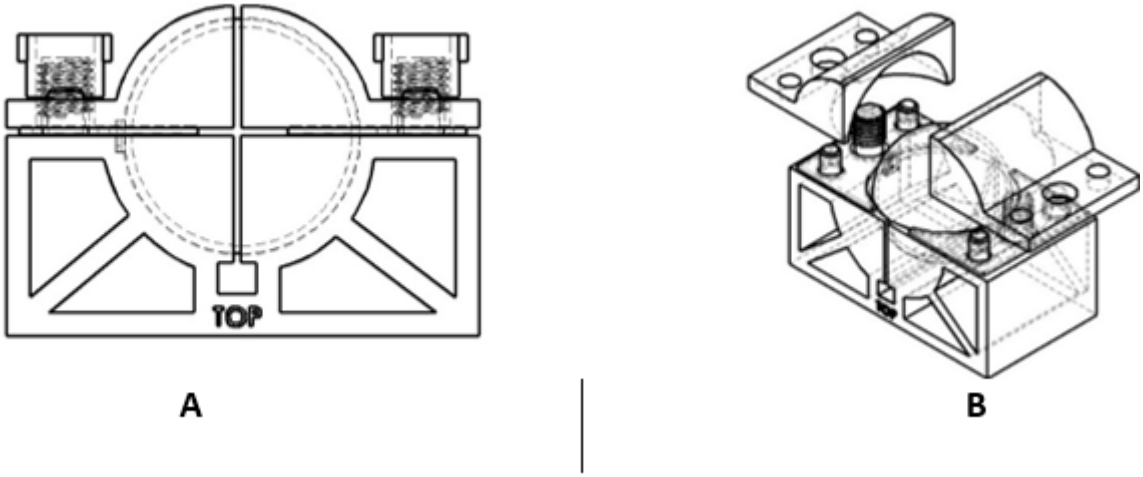

Figure 3

Cutting jig

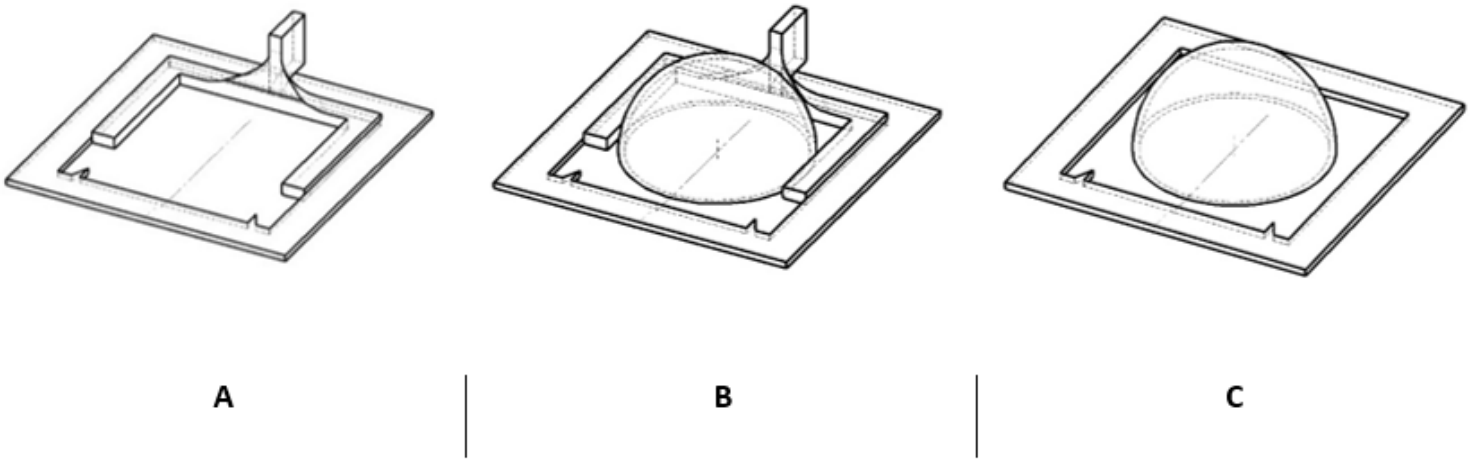

Figure 4

Measurement jig and alignment tool

Figure 4 Resins					
Curing Interval:	100%	200%	300%	400%	500%
Figure 4 MED-WHT 10 *(A)*	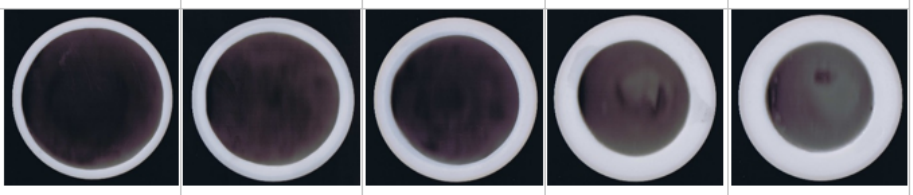				
Figure 4 PRO-BLK 10 *(B)*	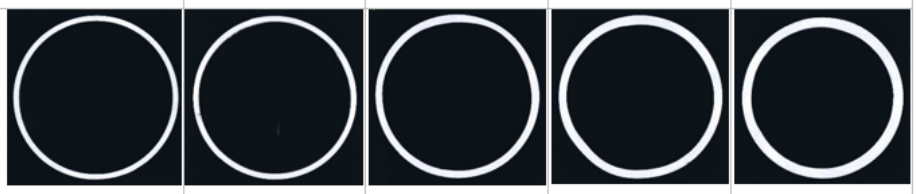				
Figure 4 MED-AMB 10 0 *(C)*		*	*	*	*
Formlabs Resins					
Curing Interval:	100%	200%	300%	400%	500%
Formlabs White Resin *(D)*	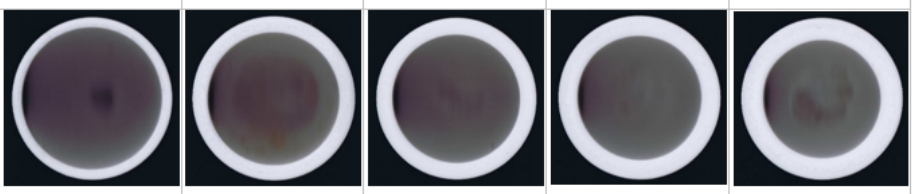				
Formlabs Black Resin *(E)*	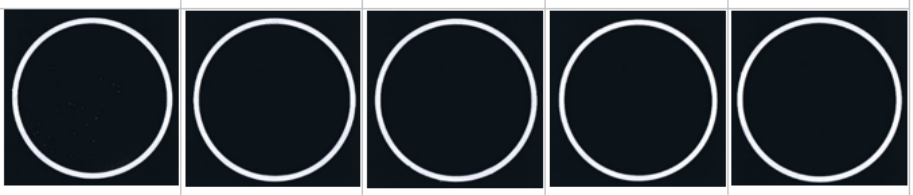				
Formlabs BioMed Amber Resin *(F)*	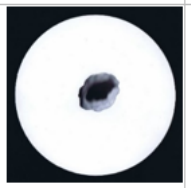	*	*	*	*

*Was not repeated as 100% interval cured to full depth

Figure 5

Scans of sectioned spheres

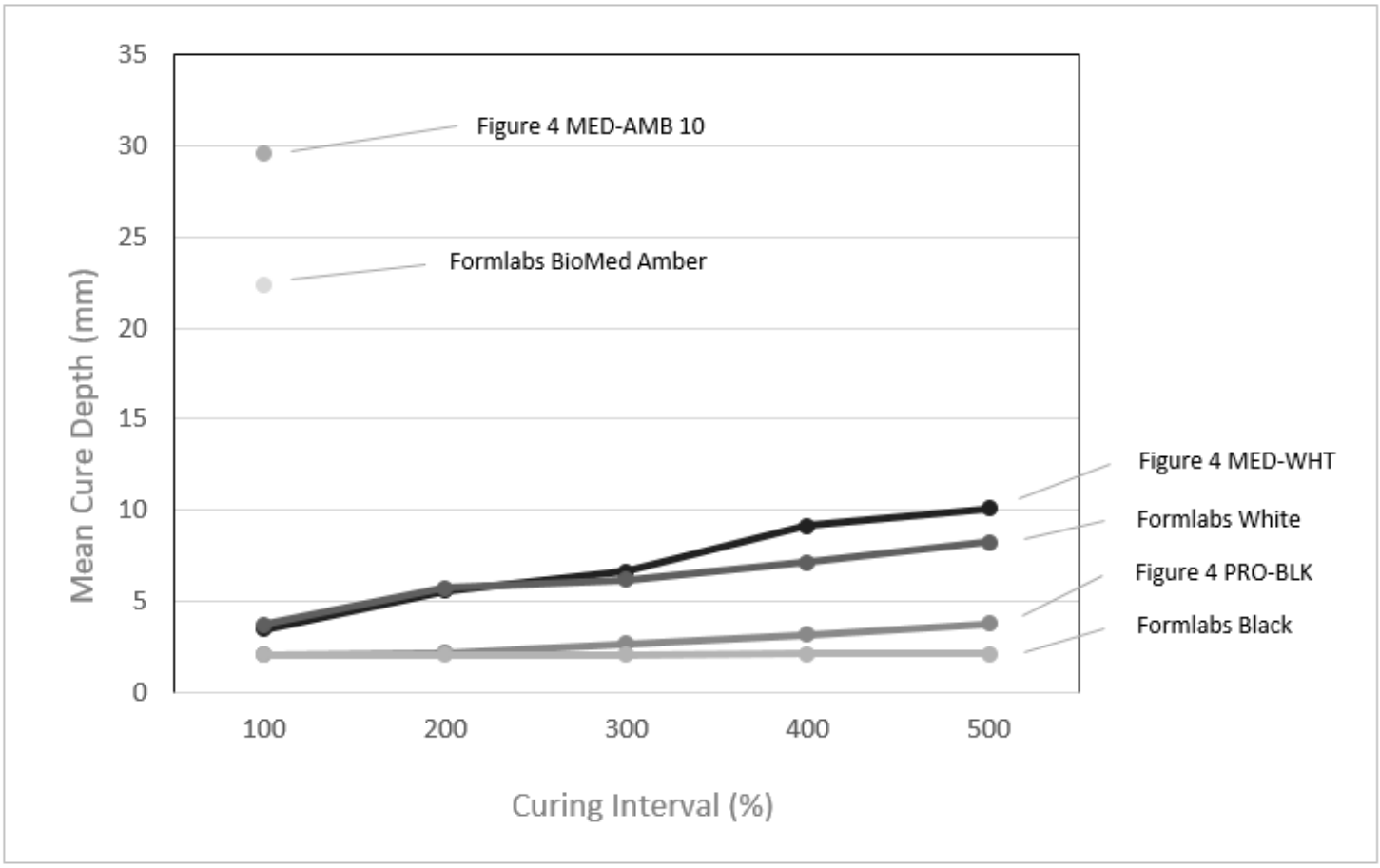

Figure 6

Mean curing depth of all resins

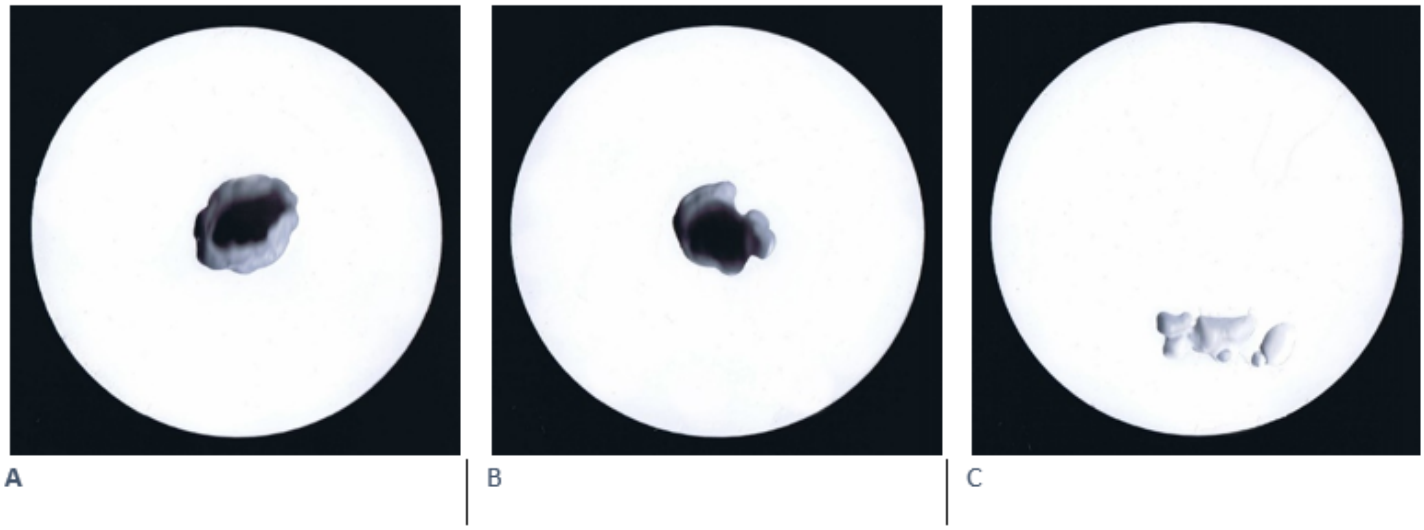

Figure 7

Biomed amber cavitation